



Biological Activity and Antitumor Studies of Some Metal Complexes with O,N,O-Chelating Schiff's Base Ligand

Abeer A. Faheim^a, Dalia I. Saleh^b, Amal M. Al-Khudaydi^b,

^aChemistry Department, Faculty of Science (Girl's), Al-Azhar University, Nasr-City, Cairo, Egypt, P.O. Box 11754,

^bChemistry Department, Faculty of Science, Taif University, Saudi Arabia.

Received 11th January 2019, Accepted 16th April 2019

Abstract

New metal complexes of Schiff base ligand derived from isatin and 4-aminoantipyrine (IAAP) with Co(II), Cu(II) and Ce(III) were prepared, and characterized by analytical and different spectroscopic techniques. On the basis of these characterizations, it was revealed that Schiff base ligands acts as a neutral tridentate ONO with octahedral geometry around metal ion. The synthesized Schiff base and its metal complexes were tested for their antibacterial, antifungal, and cytotoxic activities. The activity data show that metal complexes possessed a broad spectrum of activity against some investigated microbial species and potent cytotoxicity effect against growth of colon carcinoma cell (HCT-116) and Mouse Myelogenous leukemia carcinoma (M-NFS-60) compared to (IAAP) ligand. Moreover, the corrosion inhibition of carbon steel in HCl by some metal complexes using weight loss method was tested indicating that the metal complexes can act as corrosion inhibitors.

Key words: Schiff base; complexes; characterizations; corrosion inhibition, antimicrobial activity, antitumor cytotoxicity.

© Copy Right, IJRRAS, 2021. All Rights Reserved.

Introduction

Schiff bases derived from an amino and carbonyl compound are an important class of ligands that coordinate to metal ions via azomethine nitrogen and have been studied extensively. Schiff's bases have been widely used as ligands because they form highly stable coordination compounds and have good solubility in common solvents. These Schiff's base metal derivatives have considerable interest in biological systems, contributing to the knowledge of their structure and behavior in various activities [1]. In azomethine derivatives, the C=N linkage is essential for biological activity, several azomethine have been reported to possess remarkable antibacterial, antifungal and anticancer activities [2].

Isatin has been known for about 150 years and has been recently found, like oxindole and endogenous polyfunctional heterocyclic compounds, to exhibit biological activity in mammals [3]. Isatin also is a synthetically versatile substrate that can be used to prepare a large variety of heterocyclic compounds, such as indoles and quinolines, and as a raw material for drug synthesis [4]. Schiff bases of isatin are known to possess a wide range of pharmacological properties including antibacterial [5], anticonvulsant [6], antifungal [7]. Bis-Schiff bases are characterized by their capacity to completely co-ordinate a metal ion, forming chelate rings [8]. The Schiff bases of isatin have also been used as ligands for complexation of metals such as copper II [2]. These complexes catalyzed the oxidation of carbohydrates. Bis-Schiff bases can act as inhibitors of human α -thrombin. Recently it has been reported that a bis-imine of isatin has antimicrobial properties and affects cell viability [7].

Now a day's chemists are very much focused on the

Correspondence Author

Dr. Abeer A. Faheim Chemistry Department,
Faculty of Science (Girl's), Al-Azhar University, Nasr-
City, Cairo, Egypt, P.O. Box 11754,

Schiff bases derived from heterocyclic ring with carbonyl compounds as its important special center of attraction in many areas like biological, clinical, medicinal, analytical and pharmacological field. Among them 4-aminoantipyrine based heterocyclic had a great importance as it is abundant in nature and have wide pharmacological activities, is used in the preparation of azo dyes. 4-aminoantipyrine also has been used for the protection against oxidative stress as well as prophylactic of some diseases including cancer, and these are important directions in medical applications. Several derivatives of antipyrine were also evaluated as analgesic, anti-inflammatory, antimicrobial, and anticancer activity [9-12]. These are also strong inhibitors of cyclooxygenase isoenzymes, platelet thromboxane synthesis, and prostanooids synthesis, which catalyze the rate-limiting step of prostaglandin synthesis. Aminoantipyrine derivatives are commonly managed intravenously to detect liver disease [15] in clinical treatment. Thorough literature survey reveals that more attention has been given to Schiff's base and metal complexes derived from 4-aminoantipyrine with several aldehydes [9]. The carbonyl group in 4-aminoantipyrine is a potential donor due to the large dipole moment and strong basic characters. Since 4-aminoantipyrine has an additional potential coordination site in the amino nitrogen, it was considered worthwhile to study the complexes of this ligand [10].

2. Experimental.

2.1. Analysis and Physical Measurements

All chemical used in the present work were of highest purity available (BDH, Fluka, Sigma or Merck products). They include: isatin, 4-aminoantipyrine, hydrated metal nitrate salts namely, $\{\text{Co}(\text{NO}_3)_2 \cdot 6\text{H}_2\text{O}$, $\text{Cu}(\text{NO}_3)_2 \cdot 3\text{H}_2\text{O}$ and $\text{Ce}(\text{NO}_3)_3 \cdot 6\text{H}_2\text{O}\}$, ethanol, methanol, distilled water, double-distilled water, phosphoric acid, acetic acid, boric acid and sodium hydroxide.

Microanalyses of carbon, hydrogen and nitrogen were performed using a Perkin-Elmer CHN 2400 elemental analyzer at Micro Analytical Center, Cairo University, Giza, Egypt. Infrared spectra of studied samples were recorded as KBr discs on a Perkin-Elmer 437 IR spectrometer covering the frequency range 400-4000 cm^{-1} at the Analytical Lab, Faculty of science chemistry department Taif University, Taif, Saudi Arabia. The ^1H -NMR and ^{13}C -NMR spectra of ligand were recorded in DMF at the Analytical Center, King Abdul-Aziz University, Jeddah, Saudi Arabia. The solid reflectance measurements were measured at room temperature in the UV-Vis. regions in the wavelength (200-800 nm) were made with UV-VIS-NIR shimadzu 310 Pc, at the Analytical Center, King Abdul-Aziz University, Jeddah, Saudi Arabia. The thermo gravimetric analyses (TGA) were carried out in dynamic nitrogen atmosphere (20 mL min^{-1}) with a heating rate of 10 $^\circ\text{C min}^{-1}$ and temperature range 20-1000 $^\circ\text{C}$ using shimadzu TG-50 H and DTA-60 H thermal analyzers at Analytical Lab, Faculty of science chemistry department Taif University, Taif, Saudi Arabia. Magnetic

susceptibilities were measured by the Gouy method at room temperature using a Johnson Matthey, alfa product; model MKI magnetic susceptibility balance at the Micro Analytical Center, Cairo University, Giza, Egypt. Melting or decomposition point was measured by electronic melting point apparatus : Griffin & George made in Britain.

2.2. Synthesis of the organic ligand.

An ethanoic solution of (20 mL) of 4-aminoantipyrine (0.01 M, 2.03 gm.) was added to a solution of (0.01 M, 1.47 gm.) isatin dissolved in (20 mL) of ethanol. The mixture was refluxed for 4 hours on water bath and a red solid compound was separated.

2.3. Synthesis of the metal complexes.

The metal complexes were synthesized by an ethanoic solution of (5.0×10^{-3} M) of ligand was added to an aqueous solution of (5.0×10^{-3} M) of the hydrated metal nitrate salts. The reaction mixture was refluxed for 6 hrs. under stirring at room temperature.

2.4. Corrosion inhibition study.

The corrosion inhibition of the compounds was tested on carbon Steel rod of area 0.35 cm^2 at 25 $^\circ\text{C}$.

2.5. Assessment of antimicrobial activity.

The potential antimicrobial effects of (IAAP) and its Co(II), Cu(II) and Ce(III) complexes were investigated by using modified disc diffusion method [13] at the Regional Center for Mycology and Biotechnology Al-Azhar University, Cairo, Egypt. Two Gram-positive bacteria, namely *Streptococcus pneumonia* and *Bacillus subtilis* and two Gram-negative bacteria, namely *Salmonella typhi* and *Escherichia coli*; these bacterial strains were chosen as they are known human pathogens [14] in addition to two fungi, namely *Aspergillus fumigatus*, and *Geotricum candidum* were used in the study. Ampicillin and Amphotericin B were used as positive reference standards for bacteria and fungi, respectively to evaluate the potency of the test compounds under the same conditions while negative controls were prepared by using TFA. Briefly, 100 μL of the test bacteria / fungi were grown in 10 mL of fresh media until they reached a count of approximately 108 cells / mL for bacteria or 105 cells / mL for fungi. 100 μL of microbial suspension was spread onto agar plates corresponding to the broth in which they were maintained. Bacterial cultures were grown on nutrient broth Mueller Hinton-Agar medium at 37 $^\circ\text{C}$ for 24 hrs. and the fungal cultures were grown on Doxs medium broth at 28 $^\circ\text{C}$ for 48 hrs. The antibacterial and antifungal activities were done at one concentration; (1 mg / mL) and the diameters of inhibition zones generated by the tested samples were measured in millimeters. To ensure that the solvent had no effect on bacterial growth, a control test was performed with a test medium supplemented with TFA following the same procedures as used in the experiments.

2.6. Antitumor assays.

Potential cytotoxicity of the compounds under study

towards human colorectal cancer cells (HCT-116) was tested using method of Vijayan et al. [15] at the Regional Center for Mycology and Biotechnology Al-Azhar University, Cairo, Egypt. In brief, the cells were seeded in 96-well plate at a cell concentration of (1.0×10^4) cells per well in 100 μ L of growth medium. Fresh medium containing different concentrations of the test sample was added after 24 hrs. of seeding. The microtitre plates were incubated at 37 °C in a humidified incubator with 5% CO₂ for a period of 48 hrs.

All experiments were carried out in triplicate. After incubation of the cells for 24 hrs. at 37 °C, various concentrations of the test samples (50, 25, 12.5, 6.25, 3.125 and 1.56 μ g / mL) were added and the incubation was continued for 48 h and viable cells yield was determined by a colorimetric method. For each well, the crystal violet solution (1 %) was added for at least 30 minutes. The stain was removed and the plates were rinsed using tap water until all excess stain is removed. Glacial acetic acid (30 %) was then added to all wells and mixed thoroughly and then the absorbance of the plates was measured after gently shaken on micro plate reader using a test wavelength of 490 nm. All results were corrected for background absorbance detected in wells without added stain. Treated sample were compared with the cell control in the absence of the tested compounds.

3. Results and discussion.

All the synthesized metal complexes were found to be coloured, nonhygroscopic in nature, stable in air. The metal complexes were found to be insoluble in water, but soluble in chloroform, DMF and DMSO. The melting point of the complexes were found to be > 300 °C Table 1.

3.1. Molecular formula of metal complexes.

The results of complexes micro analytical data as well as metal estimations for the metal complexes are in good agreement with expected molecular formula assigned to these complexes Table 1, suggesting 1:1 metal ligand stoichiometric ratio, Figure (1) .

3.2. Infrared spectra and nature of coordination.

The data of the IR spectra for the Schiff base ligand and its metal complexes are listed in Table 2, Figure (2). The IR spectra of the complexes were compared with those of the free ligand to determine the involvement of coordination sites in chelation. Characteristic peaks in the spectra of the ligand and complexes were considered and compared.

The assignment of the infrared bands show the absence of (C=O) and (N-H₂) stretching vibration of isatin and 4-aminoantipyrine respectively in the spectra of ligand (IAAP), indicating the occurrence of Schiff base condensation and formation of the proposed structure of ligand. The ligand showed broad band around 1724 cm⁻¹, which are attributed to the ν (C=O) of antipyrine molecule. A sharp band at 1680 cm⁻¹ is assigned to the ν (C=O) of isatin system. Upon complexation, the ν (C=O) of the antipyrine molecule has shifted to lower frequency region, suggesting that carbonyl group is coordinated to the metal ion. Carbonyl stretching frequency of the isatin moiety at 1680 cm⁻¹ has been lowered by 60-70 cm⁻¹ in the spectra of metal complexes. This clearly indicates the coordination of the carbonyl group to the metal ion. The spectra of the ligand show the characteristic ν (C=N) band at 1540 cm⁻¹. In the spectra of the complexes, this band appears at lower frequency region indicating the coordination of the azomethine atom to the metal ion [15]. The ligand acts as tridentate-chelating agent coordinated to the metal ion via the one nitrogen ν (C=N) and two oxygen atoms. Moreover, ligand (IAAP) have shown sharp band at 3456 cm⁻¹ which are the characteristic features of the -NH of isatin molecule [17-19]. Presence of band around 3400 cm⁻¹ in the complexes of Co(II), and Cu(II) complexes is the indication of coordinated / lattice celled water molecule [20]. The bands appearing in the region 1742-1704 cm⁻¹ attributed to the coordinated NO₃ vibration while the bands appearing in the region 1484 and 748 cm⁻¹ were usual modes of phenyl ring vibration [21], while that at 2850 cm⁻¹ for the (CH₃) stretching vibrations of methyl group [22]. The presence of new bands in lower frequency region and 505-490 cm⁻¹ and 695-628 cm⁻¹ may be attributed to ν (M-N) and ν (M-O) bands, respectively [23].

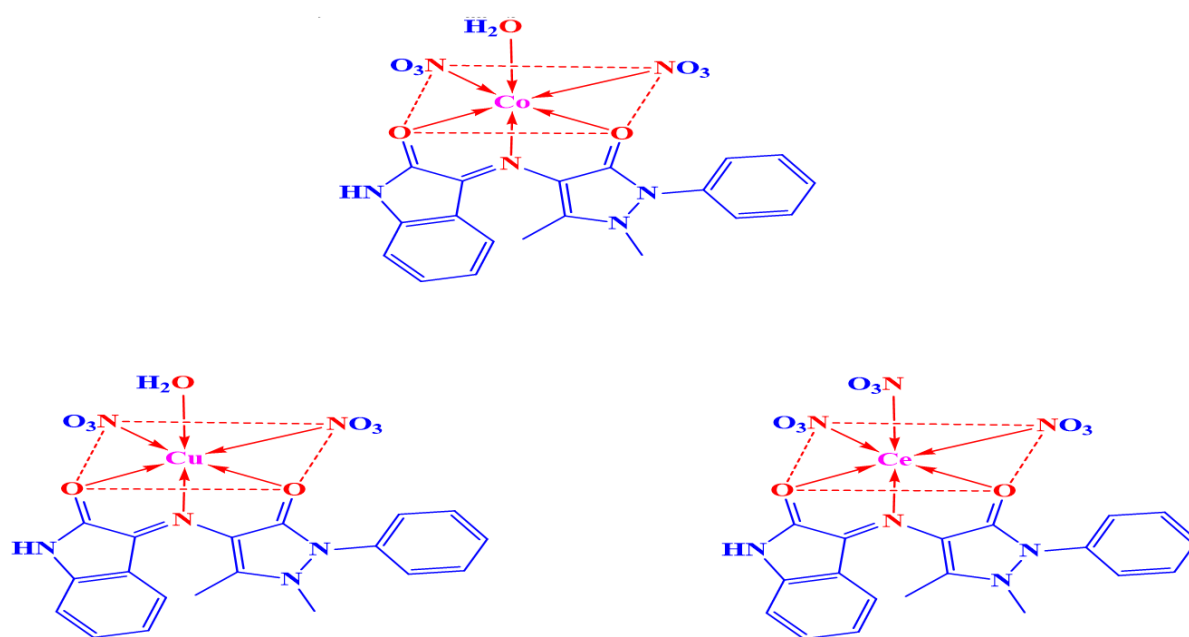


Figure (1): Suggested structure of (IAAP) Complexes.

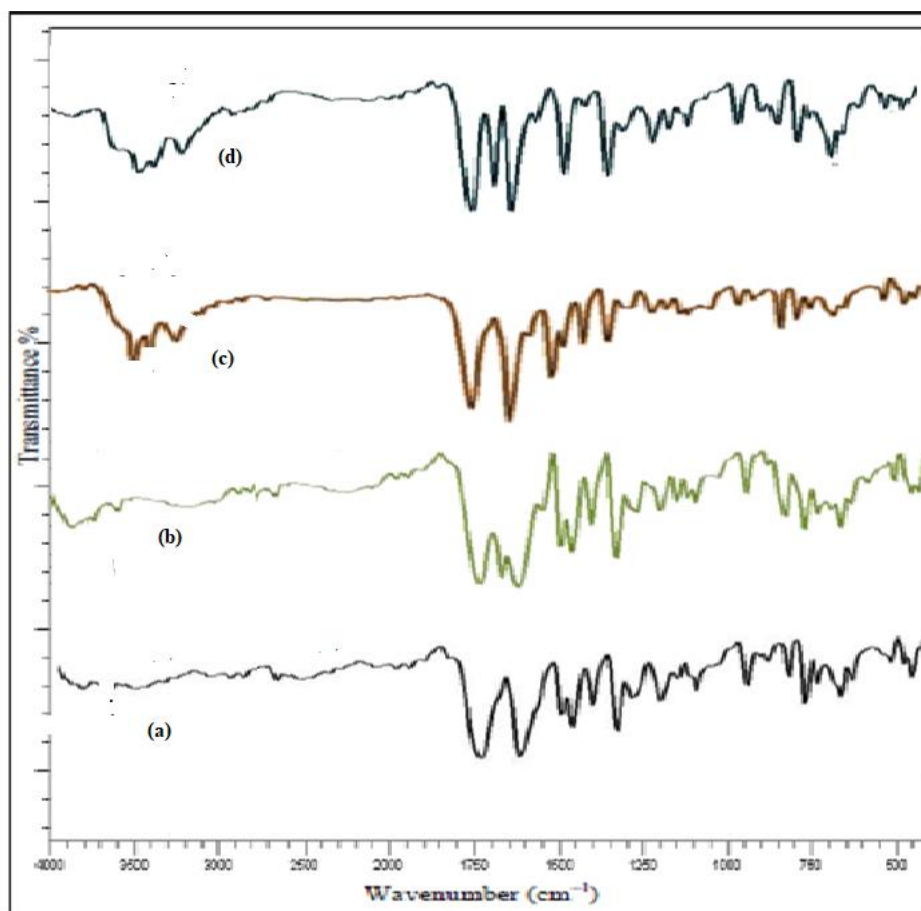


Figure (2): IR spectra of IAAP ligand and its metal complex.

(a) ligand(IAAP) (b) Co-complex
(c) Cu-complex (d) Ce-complex

Table (1): Analytical data and some physical properties of the synthesized metal complexes.

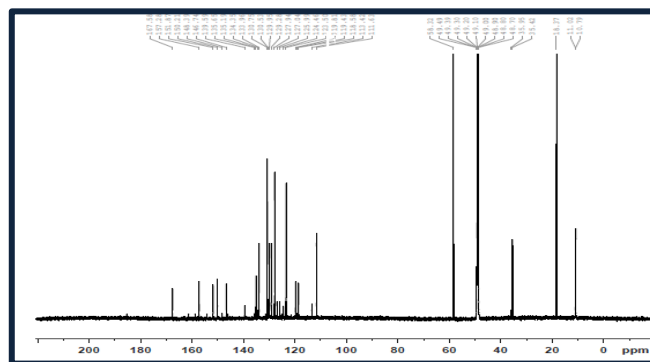
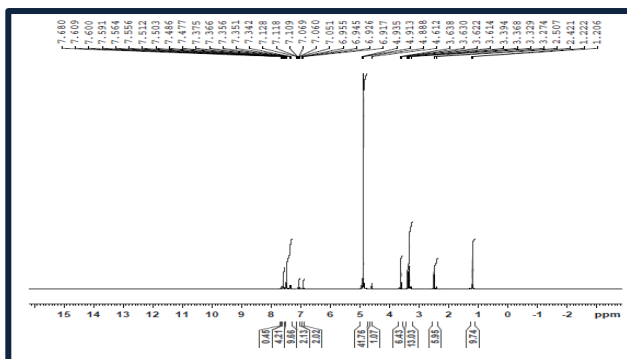
Comp. Empirical formula	Color	M. wt.	Yield %	M. p. °C	Elemental analysis, found (calc.%)			
					C	H	N	M
(IAAP) L [C ₁₉ H ₁₆ N ₄ O ₂]	Reddish Orange	332.349	88 %	179	68.756 (68.66)	5.2 (4.85)	16.34 (16.87)	-----
[Co L (NO ₃) ₂ H ₂ O] [CoC ₁₉ H ₁₈ N ₆ O ₉]	Dark Brown	533.307	85 %	>300	42.48 (42.79)	3.12 (3.40)	15.86 (15.76)	10.88 (11.05)
[Cu L (NO ₃) ₂ H ₂ O] [CuC ₁₉ H ₁₈ N ₆ O ₉]	Dark Green	537.920	85 %	>300	42.64 (42.42)	3.11 (3.38)	15.29 (15.62)	10.95 (11.81)
[Ce L (NO ₃) ₃] [CeC ₁₉ H ₁₆ N ₇ O ₁₁]	Reddish Brown	658.479	83 %	>300	34.47 (34.66)	2.61 (2.45)	14.592 (14.89)	-----

Comp.	ν (C=N) (Azomethine)	ν (C=O) (Isatin)	ν (C=O) (Antipyrine)	ν (M-O)	ν (M-O)	ν (NO ₃) Coordinated
Ligand (IAAP)	1540	1680	1724	---	---	---
[Co L (NO ₃) ₂ H ₂ O]	1505	1616	1685	683, 631	683, 631	1745, 1714
[Cu L (NO ₃) ₂ H ₂ O]	1504	1624	1684	652, 627	652, 627	1731, 1708
[Ce L (NO ₃) ₃]	1498	1608	1686	685, 634	685, 634	1722

3.3. The ¹H-NMR and ¹³C-NMR spectra.

The ¹H-NMR and ¹³C-NMR spectra of ligand were recorded in DMF. In the ¹H-NMR spectrum of the ligand (IAAP) Figure (3). The multiple peaks around 7-8 ppm is attributed to aromatic proton. The spectrum exhibit multiple signals at 2-3 ppm which may be assigned to protons of methyl groups (C-CH₃) and (N-CH₃), which are attached to the pyrazolone ring. The spectrum displays another multiple in the range at 6.9-7.1 ppm which may be due to the protons of isatin aromatic ring. Figure (4),

presents information on the ¹³C-NMR of the ligand, the signals at 10.79 and 35.42 ppm are due to carbon atoms of methyl groups attached to the pyrazolone rings (C-CH₃ and N-CH₃). The two kinds of C-atoms of pyrazolone rings (Me-C and N-C) give signals at 134.35 and 139.59 ppm. The signals at 157.28 ppm due to (C=O) group and the 6 signals at 127.04-130.65 ppm due to six C-atoms of aromatic ring. Isatin (C=O) appeared in 167.58 ppm and the signals at 146.74 ppm is assigned to (C=N).

**Figure (3): ¹H-NMR spectrum of the ligand.****Figure (4): ¹³C-NMR spectrum of the ligand.**

3.4. Electronic spectra and magnetic moment.

The nature of the ligand field around metal ion has been deduced from the electronic spectra. The electronic spectral data of the complexes are tabulated in Table 3. The electronic spectrum of free Schiff base showed a band

around 240 and 341 nm characteristic of $\pi-\pi^*$ and $n-\pi^*$ transitions, respectively. In the metal complexes, $n-\pi^*$ band is shifted to a longer wave length with increasing intensity. This shift may be attributed to the donation of the lone pair of electrons of nitrogen of Schiff base to metal ion, i.e. ligand to metal charge transfer (LMCT) bands. The visible spectra of Co(II) complex has shown the band around 410 nm which is attributed to the LMCT. In addition to this, complex displays the band at 558 nm assigned to d-d transition. The magnetic moment value of

Co(II) complex μ_{eff} 5.13 B.M. which corresponds to three unpaired electrons and that agree with octahedral configuration. The Cu(II) complex has shown the band around 418 nm which is attributed to the LMCT. In addition to this, complex displays the band at 559 nm assigned to d-d transition. The magnetic moment value of Cu(II) complex μ_{eff} 1.77 B.M. That agree with octahedral configuration. The Ce(III) complex has shown the band around 458 nm which is attributed to the LMCT. The magnetic moment value of Ce(III) complex μ_{eff} 1.87 B.M.

Table (3): The electronic spectra of the ligand and their complexes.

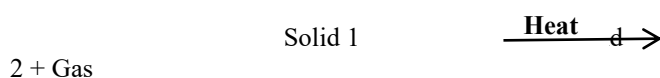
Comp.	$\pi - \pi^*$	$n-\pi^*$	Charge transfer transition	d-d transition	μ_{eff} B.M	Molar conductance	Expected structure
Ligand (IAAP)	210	254, 325	---	---	---	---	---
Co-Complex	212	284, 375	410	558	5.13	7.3	Octahedral
Cu-Complex	220	274, 384	418	559	1.77	5.3	Octahedral
Ce-Complex	222	275, 388	430	----	1.87	7.5	Octahedral

3.5. Thermo gravimetric analysis.

The thermal methods of analysis are widely used to investigate, thermal decomposition, thermal stability, solid state reactions, purity, reaction kinetics, evolved gas analysis as well as to verify the status of associated water / solvent into inside or outside the inner coordination sphere of the central metal ion supports the elemental analyses and confirms the structure of the metal complexes [24-27].

The thermo gravimetric analysis (TGA) of (IAAP) and its Co(II), Cu(II) and Ce(III) complexes Figure (5), Table 4 are showed that the temperature range ($^{\circ}\text{C}$), partial mass losses (%) together with the assignments of each decomposition step based on mass calculation and nature of the peaks in each stage of decomposition. In all the (TG / DTG) curves, the results show good agreement with the calculated formulas as suggested from the analytical data Table1.

The successive solid products of decomposition were obtained at temperatures determined on the basis of the (TG) curves. Each step of decomposition in most of the reactions of the solids follows the trend:



This process comprises several stages, such as the chemical act of breaking bonds, breakdown of the crystal lattice of solid 1, formation of the crystal lattice of the solid 2, diffusion of gas and heat transfer [28,29]. Additionally, the thermogram curves exhibit a series of thermal changes during the increase of temperature and the most important observation is that, in all investigated

Co(II), Cu(II) and Ce(III) complexes no weight loss was observed upon heating till 138°C , and thus, ruling out the presence of hydrated water molecules associated physically with the complex sphere which proposed mainly based on the elemental analysis as well as the IR data [30].

The thermo gram of Co(II) complex shows weight loss 14.406 % corresponding to one water molecule, N_2 and O_2 molecules in the range $138-292^{\circ}\text{C}$. The loss of water in this temperature range indicates the presence of water molecule in the coordination sphere of Co(II) complex [31]. Decomposition reaction corresponds to an experimental mass 27.941 % occurs in the temperature range $292-380^{\circ}\text{C}$ attributed loss of isatin moiety [32] part of the complex. In the temperature range $380-533^{\circ}\text{C}$ aminoantipyrine moiety and carbonyl part is lost and this loss corresponds to 44.931 %. Finally, residue is obtained corresponding (CoO) as stable residue [33].

The TGA of Cu(II) complex indicates 14.409 % loss in weight in the range $167-285^{\circ}\text{C}$ corresponding to one water molecule and N_2 molecule. Isatin undergoes decomposition in single stage between the temperature range $295-470^{\circ}\text{C}$ and 27.205 % weight loss was observed. In the temperature range $470-680^{\circ}\text{C}$ aminoantipyrine moiety is lost and this loss corresponds to 45.121 percent. the residue about 14.8 %.

The TGA of Ce(II) complex indicates 22.780 % loss in weight in the temperature range $310-490^{\circ}\text{C}$ corresponding to decomposition of Isatin moiety. In the temperature range $490-690^{\circ}\text{C}$ aminoantipyrine moiety is lost and this loss corresponds to 47.701 %. the residue obtained is metal oxide.

Table (4): Thermo gravimetric analyses (TGA) results of the (IAAP) complexes.

Empirical formula	Temp. range (°C)	Weight loss% Found(Calc.)	Evolved moiety	Composition of the residue
[Co L (NO ₃) ₂ H ₂ O] [CoC ₁₉ H ₁₈ N ₆ O ₉]	Stage I: 138-292 Stage II: 292-380 Stage III: 380-433	14.406 (14.63) 27.941 (27.20) 44.931 (44.47)	H ₂ O (coord.) and N ₂ O ₂ C ₈ H ₅ N ₂ O (isatin moiety) C ₁₁ H ₁₃ N ₂ O ₄	[CoC ₁₉ H ₁₆ N ₄ O ₆] [CoC ₁₁ H ₁₃ N ₂ O ₅] CoO
[Cu L (NO ₃) ₂ H ₂ O] [CuC ₁₉ H ₁₈ N ₆ O ₉]	Stage I: 167-285 Stage II: 295-470 Stage III: 470-680	14.409 (14.52) 27.205 (26.95) 45.121 (44.05)	H ₂ O (coord.) and N ₂ O ₂ C ₈ H ₅ N ₂ O (isatin moiety) C ₁₁ H ₁₃ N ₂ O ₄	[CuC ₁₉ H ₁₆ N ₄ O ₆] [CuC ₁₁ H ₁₃ N ₂ O ₅] CuO
[Ce L (NO ₃) ₃] [CeC ₁₉ H ₁₆ N ₇ O ₁₁]	Stage I: 310-490 Stage II: 490-690	22.780 (22.035) 47.701 (47.445)	C ₈ H ₅ N ₂ O (isatin moiety) C ₁₁ H ₁₁ N ₅ O ₇	[CeC ₁₁ H ₁₁ N ₅ O ₁₀] Ce ₂ O ₃

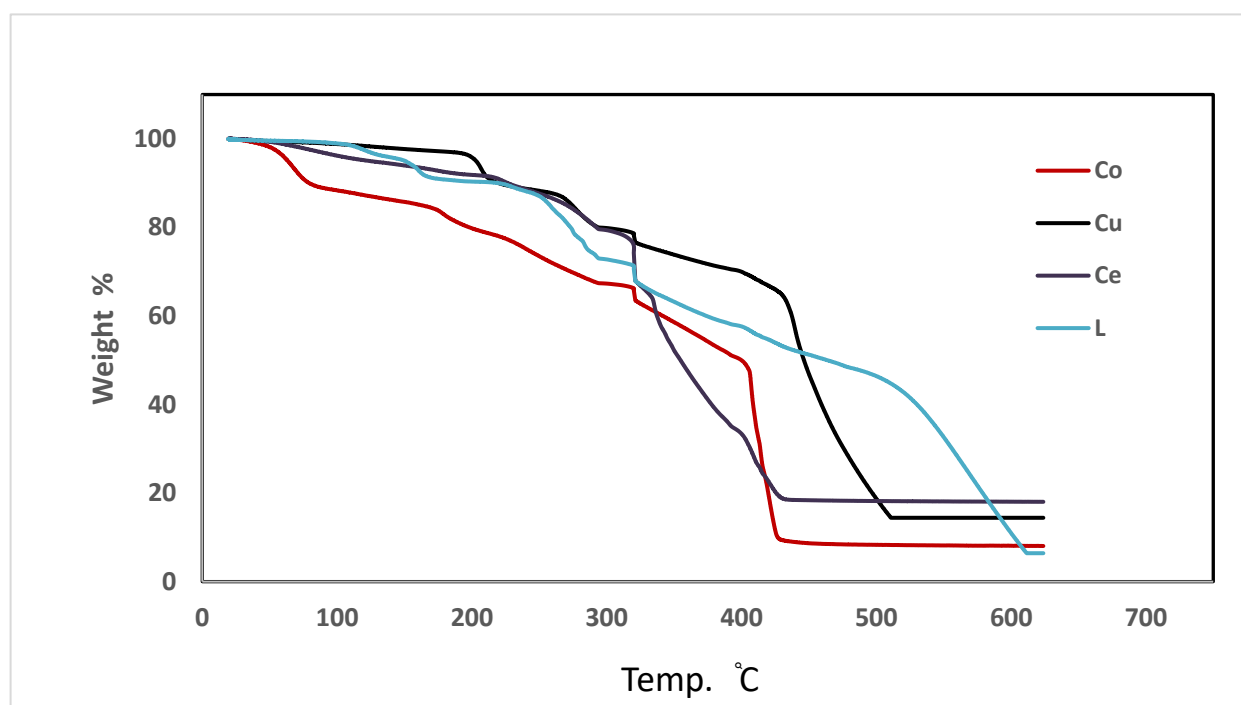


Figure (5): TG-thermogram of the ligand (IAAP) and its metal complexes

3.5.1. Thermodynamic parameters

In order to characterize the metal complexes more fully in terms of thermal stability, their thermal behaviors were studied, the thermodynamic activation parameters of decomposition processes of the metal complexes namely activation energy (E^*), enthalpy (ΔH^*), entropy (ΔS^*) and Gibbs free energy change of the decomposition (ΔG^*) were evaluated graphically by employing Coats–Redfern [34].

From the results obtained Table (5) and Figure (6), the following remarks can be pointed out:

- The high values of the energy of activation, E_a of the complexes reveal the high stability of such chelates due to their covalent bond character [35].
- The positive sign of ΔG^* for the investigated complexes reveals that the free energy of the final residue is higher than that of the initial compound, and all the decomposition steps are nonspontaneous processes. Also, the values of the activation, ΔG^* increases significantly for the subsequent decomposition stages of a given complex. This is due to increasing the values of $T\Delta S^*$ significantly from one step to another which overrides the values of ΔH^* [36].
- The negative ΔS^* values for the decomposition steps indicate that all studied complexes are more ordered than the reactant. [37].
- The positive values of ΔH^* mean that the decomposition processes are endothermic [38].

Table 5: Thermodynamic data of the thermal decomposition of the synthesized ligand ,L and its Complexes .

Compound	Steps	Decomposition Temp. °C	$\Delta H^\#$ (J/mol)	$\Delta S^\#$ (J/mol)	$\Delta G^\#$ (J/mol)	Ea (J/mol)
[Co L (NO₃)₂ H₂O] [CoC₁₉H₁₈N₆O₉]	I	138-292	54952	-142.3	1157445	59074
	II	292-380	105834	-90.52	161161	110919
	III	380-433	109132	-125.65	195457	114848
[Cu L (NO₃)₂ H₂O] [CuC₁₉H₁₈N₆O₉]	I	167-285	67080	-118.21	125747	71320
	II	295-470	105834	-111.25	154667	91758
	III	470-680	108791	-126.14	200619	114848
[Ce L (NO₃)₃] [CeC₁₉H₁₆N₇O₁₁]	I	310-490	72744	-146.18	169222	78235
	II	490-690	103905	-93.19	182470	110919

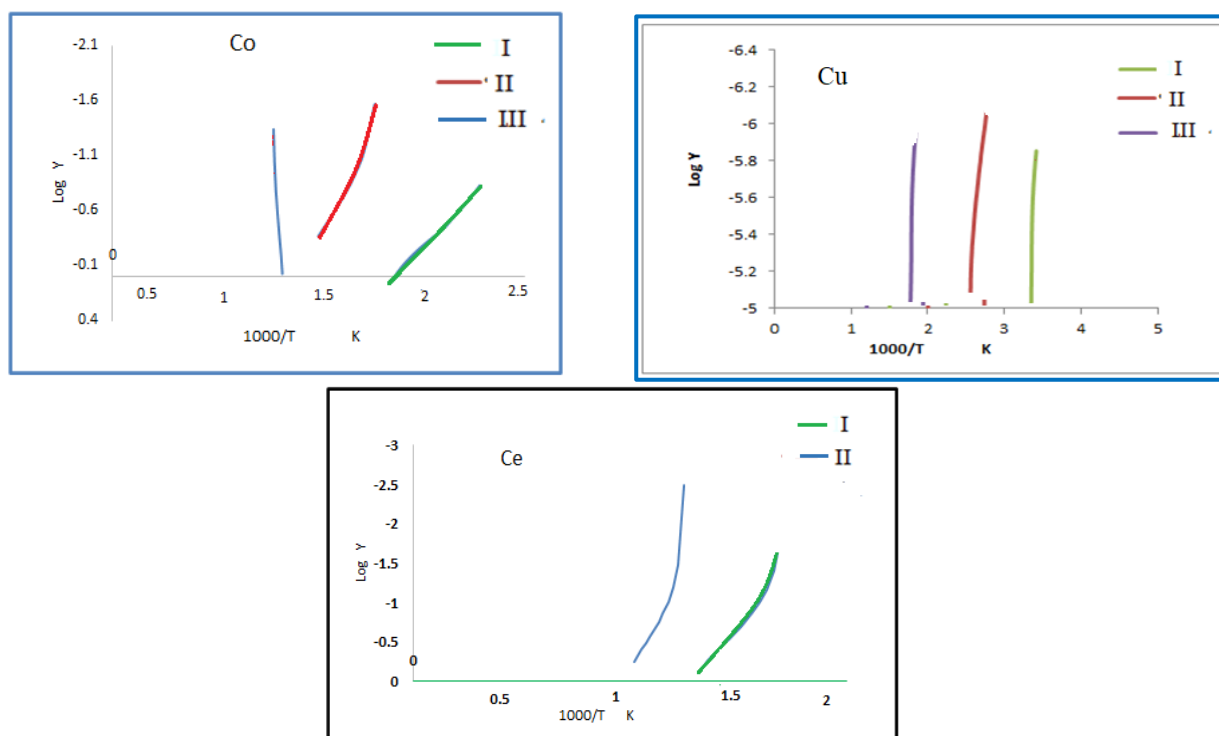


Figure (6) : Coast -Redfern plots of the synthesized metal complexes

$$* \text{Log } Y = \text{Log}[\log \{W_\infty (W_\infty - W)^{-1}\} T^{-2}]$$

3.6. Evaluation of the synthesized compounds.

3.6.1. Evaluation of the synthesized compounds as corrosion inhibitors by weight loss measurements.

The presence of O and N atoms in the ligand have an inhibition effect on steel [39-41], so we find that it has inhibition of 4.78 % after 2 hrs. and the inhibition effect increased to 10.70 % and 12.27 % after 4 and 8 hrs., respectively. Co(II), Cu(II) and Ce(III) complexes make good inhibitors on steel [42-44].

Table (6): Inhibition efficiencies of ligand and its complexes on carbon steel corrosion in 0.5M HCL at 25 °C obtained by weight loss method.

2	Rate $\times 10^{-2}$	9.00	8.57	7.80	7.00	7.20	4.50
	%inhibition	-	4.78	13.33	22.22	20.0	35
4	Rate $\times 10^{-2}$	7.71	6.89	6.00	5.00	5.77	3.75
	%inhibition	-	10.70	22.22	35.18	25.21	42.13
8	Rate $\times 10^{-2}$	0.63	0.56	0.379	0.365	0.375	0.273
	%inhibition	-	12.27	40.15	42.37	40.79	56.89

These metals complexes with (IAAP) ligand have an inhibition effect on the steal as given in Table 6, and shown in Figure (7) the inhibition rate is arranged as follow:

(IAAP) ligand < Co(II)-complex < Cu(II)-complex < Ce(III)-complex.

The experimental is repeated in 2, 4 and 8 hrs., we show that the inhibition rate increases with increasing time in all ligand and its complexes in the same arrangement.

(IAAP) ligand < Co(II)-complex < Cu(II)-complex < Ce(III)-complex.

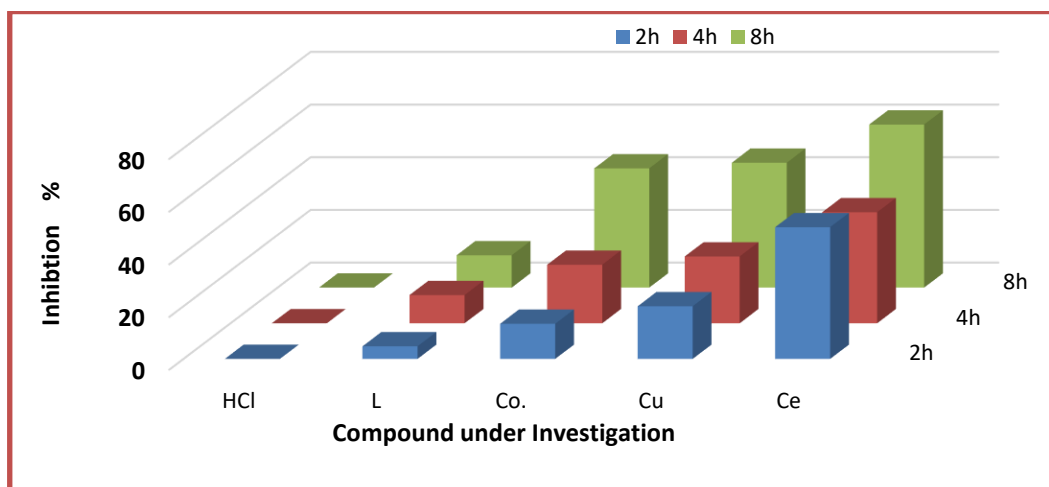


Figure (7) : Inhibition efficiency of (IAAP) and its metal complexes.

3.6.2. Evaluation of the antimicrobial activity of synthesized compounds.

The antimicrobial activities of (IAAP) and its synthesized metal complexes were tested in vitro against series of organisms to increase the chance of detecting antibiotic principles in tested materials. The activity was determined by measuring the inhibition zone diameter values (mm) of the complexes against the organisms. The screening data in addition to the calculated percent activity index are given in Table 7 and are graphically presented in Figures (8 and 9). Analyzing the tabulated results indicated that:

- 1-(IAAP) and its Co(II), Cu(II) and Ce(III) complexes, possessed a broad spectrum of activity against the sensitive organisms except *Syncephalastrum racemosum* and *Salmonella typhi* as they did not show any activity towards it. Similarly, no effect was observed for Co(II) complex, towards all sensitive organisms.
- 2- No effect was observed for (IAAP) towards all sensitive organisms and such inhibition was enhanced on complexation especially in case of Cu(II) and Ce(III) complexes, but less than the standard used.
- 3- Ce(II) complex, display high activity towards all sensitive organisms except *Candida tropicalis* and *Salmonella typhi*.
- 4- Co(II) and Cu(III) complexes, display high activity towards all sensitive organisms except *Syncephalastrum racemosum*, *Candida tropicalis* and *Salmonella typhi*.
- 5- Antimicrobial activity of the synthesized complexes is promising, so determining the minimum inhibitory concentration (MIC) for the synthesized complexes is recommended.

Table (7): Antimicrobial Screening results of (IAAP) ligand and its complexes.

Sample Tested Microorganisms	(IAAP)	Co(II)- complex	Cu(II)- complex	Ce(III)- complex	St.
Fungi					<i>Amphotericin B</i>
<i>Aspergillus Fumigatus</i> (RCMB 02568)	NA	18.3	21.3	19.2	23.7
<i>Geotricum candidum</i> (RCMB 05097)	NA	13.2	19.2	14.31	28.7
Gram positive bacteria					<i>Ampicillin</i>
<i>Streptococcus pneumonia</i> (RCMB 010010)	13.2	13.4	17.3	16.3	23.8
<i>Bacillus subtilis</i> (RCMB 010067)	15	16.3	19.2	18.4	23.4

Gram negative bacteria					Ciprofloxacin
<i>Salmonella typhi</i> (RCMB 010072)	NA	NA	11	12	22.3
<i>Escherichia coli</i> (RCMB 010052)	NA	14.6	22.3	16.1	26.2

- Test was done using the diffusion agar technique . NA: No activity .

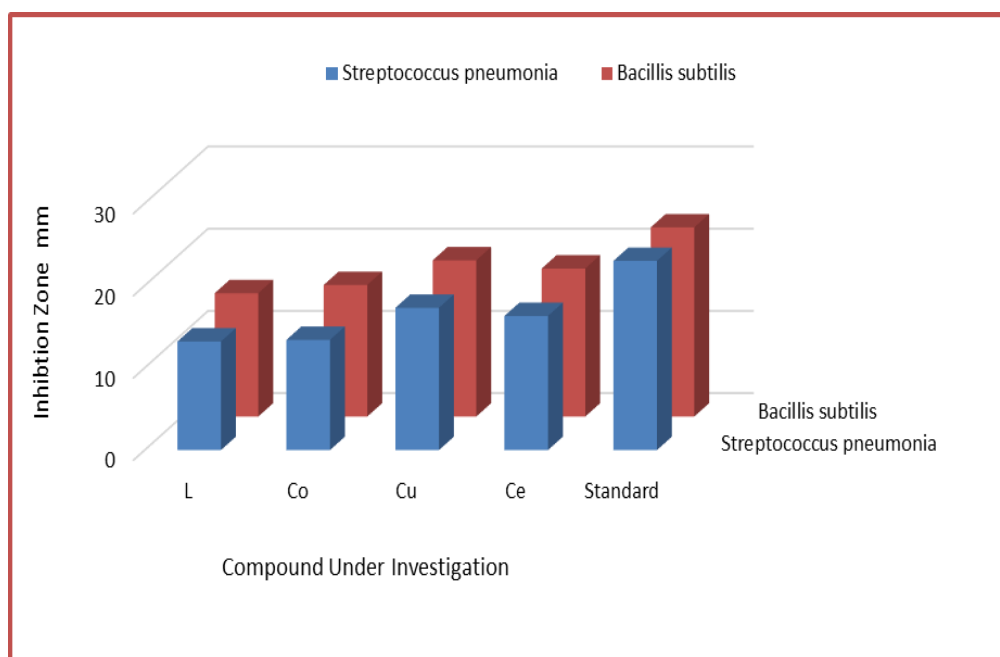


Figure (8): The antibacterial activity of (IAAP) and its metal complexes.

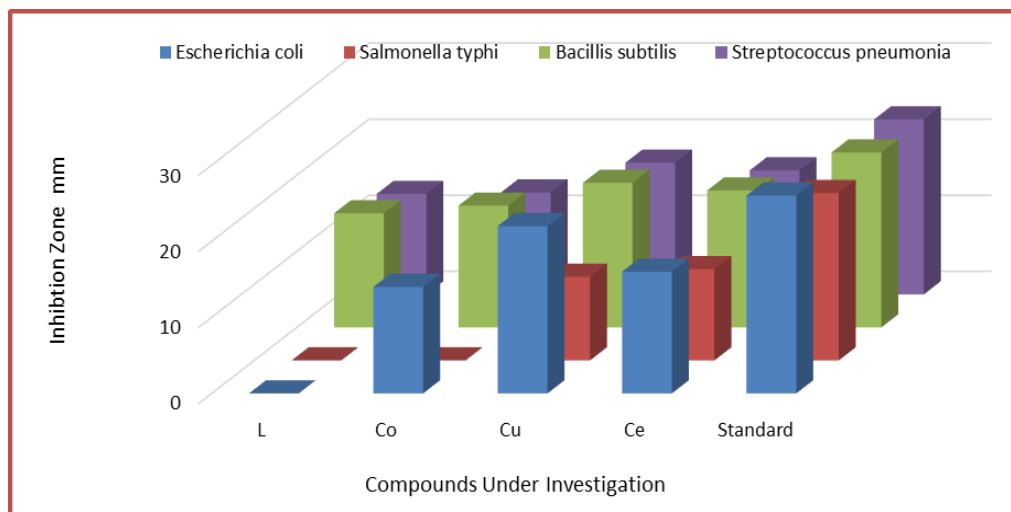


Figure (9): The antifungal activity of (IAAP) and its metal complexes.

3.2.7.3. Cytotoxicity for tumor cells.

Cancer is the second most life threatening disease after cardiovascular disease, affecting more than six million people per year worldwide. Drastic changes in life style during the end of the 19th century has increased the risk of humans developing different types of cancers. Also, considerable effort has been put into identifying molecules with anti-cancer properties from both natural and synthetic sources [45].

Colon cancer, along with breast and leukemia cancer, is one of the most prevalent cancers in the world [46]. While in

early stages, colon cancer is characterized by a good prognosis, in more advanced, metastatic stages, the five-year survival rate is only 10 %. Approximately 25 % of all colon cancer patients reach this stage and are principally treated with 5-fluorouracil (5-FU) alone or a combination of oxaliplatin (FOLFOX, a combo of oxaliplatin, 5-FU and leucovorin), angiogenesis inhibitors and /or epidermal growth factor receptor inhibitors. However, the results from current treatments are poor and may be accompanied by tissue damage.

Hence (IAAP) ligand and its metal complexes were tested for antitumor activity against colon carcinoma cell (HCT-116) and Mouse Myelogenous leukemia carcinoma (M-NFS-60) at concentration (100, 50, 25, 12.5, 6.25, 3.125 and 1.56 $\mu\text{g} / \text{mL}$). Anticancer efficiency of all the tested compounds is tabulated in Tables 8 and 9 where Figures (10 and 11) show effect of different concentration of all compounds under study on (HCT-116) and (M-NFS-60), respectively. Additionally, the IC_{50} values derived from experimental data summarized in Tables 7 and 8 and represented graphically in Figure (12).

All the metal complexes were found to be cytotoxic against (HCT-116) and (M-NFS-60) and produce 50 % cell death at concentrations range of (7.26 – 36.12 $\mu\text{g} / \text{mL}$) moreover, they show little cytotoxicity in compared to (IAAP) ligand. Among the metal complexes, Cu(II) complex with IC_{50} values (7.26 and 12.4 $\mu\text{g} / \text{mL}$) were observed to be the most active complex having the lowest IC_{50} value, additionally Ce(III) complex showed comparable effect with IC_{50} (16.9 and 21.3 $\mu\text{g} / \text{mL}$). Antitumor activity of the compounds follow the order :

Cu(II)-complex > Ce(III)- complex > Co(II)-complex > (IAAP) ligand.

For both colon carcinoma cell (HCT-116) and Mouse Myelogenous leukemia carcinoma (M-NFS-60).

Table (8): Cytotoxicity for (IAAP) and its complexes against human colorectal cancer cells (HCT-116).

Comp.	Cell viability % at different concentrations (μg)								IC_{50} ($\mu\text{g}/\text{mL}$) ^(a)
	0.0	1.56	3.125	6.25	12.50	25.00	50.00	100.0	
(IAAP)	100.00	100.00	98.92	89.37	79.42	66.25	40.87	26.48	36.34
Co(II)	100.00	100.0	96.15	80.43	69.72	43.86	30.42	21.75	22.54
Cu(II)	100.00	96.97	70.95	63.48	49.67	42.21	34.08	21.74	12.4
Ce(III)	100.00	92.12	87.59	81.78	70.92	56.43	39.74	25.58	16.9

^(a) IC_{50} is concentration which can reduce the growth of cancer cells by 50%.

Table (9): Cytotoxicity for (IAAP) and its complexes against leukemia cells (M-NFS-60).

Comp.	Cell viability % at different concentrations (μg)								IC_{50} ($\mu\text{g}/\text{mL}$) ^(a)
	0.0	1.56	3.125	6.25	12.50	25.00	50.00	100.0	
(IAAP)	100.00	98.71	94.22	89.56	74.19	57.23	49.98	34.15	48.34
Co(II)	100.00	98.82	94.56	80.19	67.24	38.71	25.86	18.72	22.40
Cu(II)	100.00	80.34	67.58	52.34	37.87	29.65	22.38	14.96	7.26
Ce(III)	100.00	95.28	90.83	78.65	59.41	32.96	26.79	21.36	21.3

^{a)} IC_{50} is concentration which can reduce the growth of cancer cells by 50%.

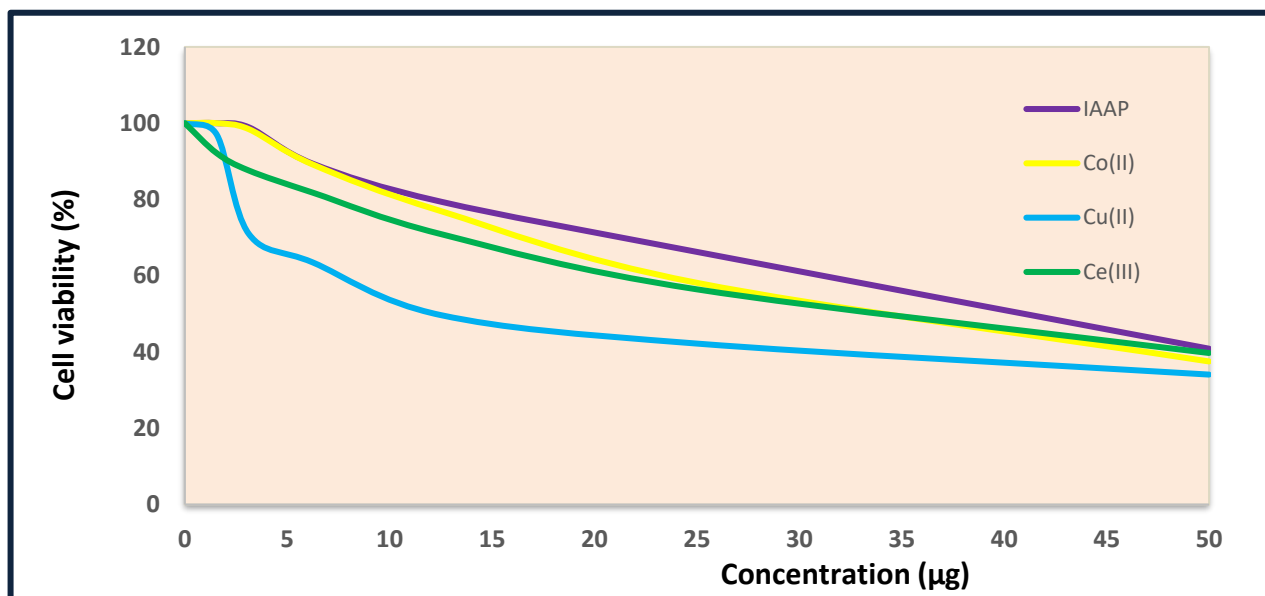
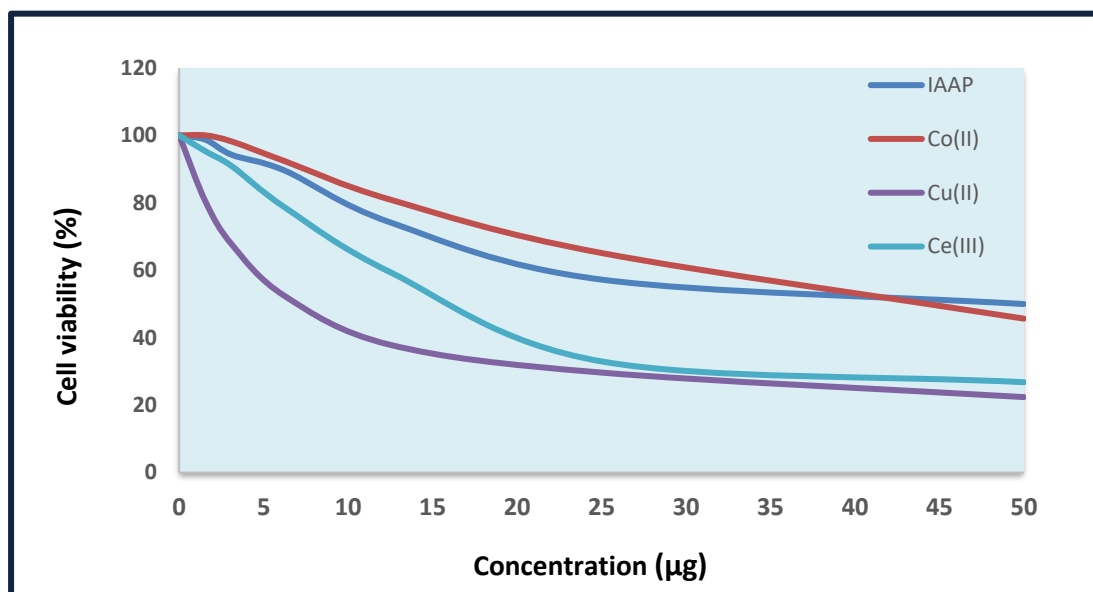


Figure (10): Antitumor activity of (IAAP) and its Co(II), Cu(II) and Ce(III) complexes against human colorectal cancer cells (HCT-116).

Figure



(11):

Antitumor activity of (IAAP) and its complexes against Mouse Myelogenous leukemia carcinoma cells (M-NFS-60).

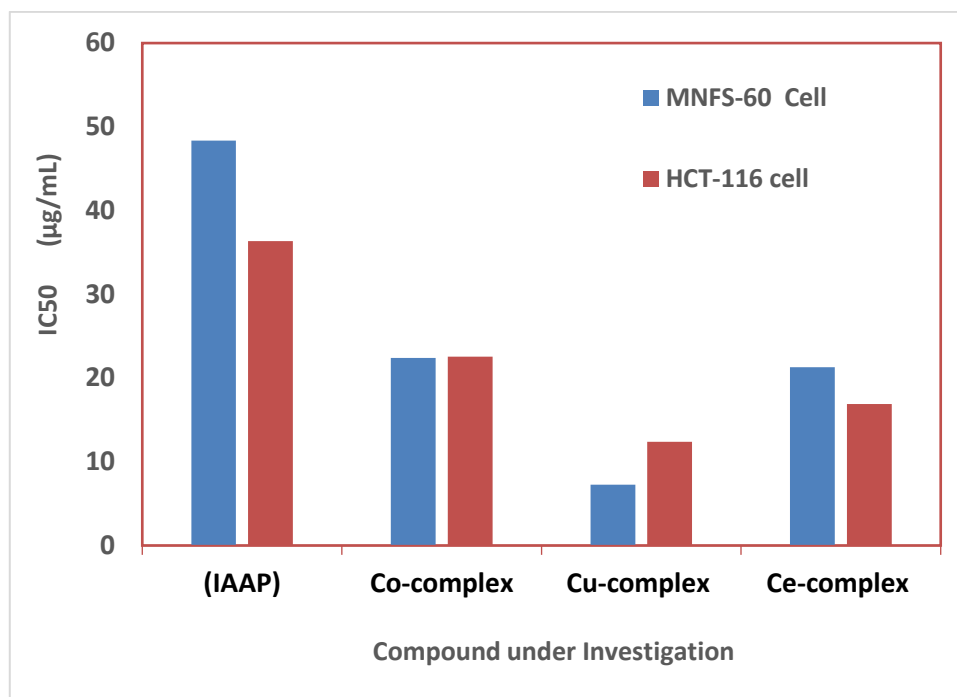


Figure (12): Variation of IC₅₀ value of (IAAP) and its complexes for (MNS-60) cells and (HCT-116 cells).

Conclusion :

In this research, we have presented the synthesis of a metal complexes derived from Schiff base ligand Isatin and 4-aminoantipyrine. The structures of the ligand and its metal complexes were confirmed by various spectral and elemental analyses. The present study suggests the coordination of the ligand to the metal ions in O, N, O fashion. All the complexes are found to be non-electrolytic in nature with octahedral geometry. The evaluation of the synthesized compound via Corrosion inhibition of carbon steel in HCl by the prepared compounds using weigh loss method was tested indicating that the metal complexes can act as corrosion inhibitors. The prepared compounds were evaluated for their antimicrobial activity and have exhibited promising activity toward the sensitive organisms. The antibacterial activity of the complexes must be investigated with further studies at different concentration. Finally, the ligand and tested complexes showed a high potential cytotoxic activity against growth of colon carcinoma cell (HCT-116) and Myelogenous leukemia carcinoma (M-NFS-60) tumor cell lines. All complexes were found to be more active than the free ligand. This indicates enhancing of antitumor activity upon coordination.

References :-

1. N. I. Shutilova and D. N. Moiseev, Protection of Metals and Physical Chemistry of Surfaces, 46 (2010) 502-507.
2. B. Singh and D. Kumar, International Journal of Scientific and Research Publications, 3(2) (2013).
3. Y. A. Mohammed. Review of Catalysts, 2 (2015) 14-25
4. Y. A. Mohammed, T. Baraki, R. K. Upadhyay, and A. Masood, American Journal of Applied Chemistry, 2 (2014)15-18.
5. C. E. Housecroft, International Journal for Chemistry, 2018. 72(1-2): p. 36-42.
6. N. Sharma, Raviprakash and K. Chaturvedi, Sci. Revs. Chem. Commun, 2(2) (2012) 108-114.
7. E. M. Jouad, G. Larcher. M. Allain. A. Riou, G. M. Bouet, M. A. Khan and X. Do Thanh, J. Inorg. Biochem., 86 (2001) 565.
8. Mir, J.M., D. Kumar Rajak, and R. Charitra Maurya, Journal of Coordination Chemistry, 2018. 71(14): p. 2225-2242.
9. L. K. Gupta, U. Bansal and S. Chandra, Spectrochimica Acta Part A, 66 (2007) 972-975.
10. Z.H. Abd El-wahab, M. M. Mashaly, and A. A. Faheim Synth. React. Inorg. Met-Org. Chem 59 (2005) 25-36.
11. M. M. Mashaly, Z. H. Abd-Elwahab and A.A. Faheim, Chinese Chem. Soc. 51(2004) 901-915.
12. N. T. Akinchan, P. M. Drozdowski and W. Holzer, J. of Mol. Structure, 641 (2002) 17-22.

13. M. Aljahdali, Spectrochim. Acta Part A, 112 (2013) 364-376.
14. P. Vijayn, C. Raghu, G. Ashok, S.A. Dhanaraj and B. Suresh, Indian J. Med. Res., 120 (2004) 24-29.
15. N. Rahman and S. N. H. Azmi, Anal. Sci., 16 (2000) 1353.
16. T. Atalay and E. Akgemci, Tr. J. Chem., 22 (1998) 123.
17. P. Lampman, Kriz and Vyvyan, Introduction to spectroscopy (fourth edition), Brooks/Cole CENGAGE Learning, (2007).
18. S. Sarkar, S. Biswas, M.S. Liao, T. Kar, Y. Aydogdu, F. Dagdelen, G. Mostafa, A.P. Chattopadhyay, G.P.A. Yap, R.H. Xie, A.T. Khan and K. Dey, Polyhedron, 27 (2008) 3359-3370.
19. M. Tuncel, A. Ozbulbul and S. Serin, Reactive & Functional Polymers, 68 (2008) 292-306.
20. S. Ilhan, H. Temel, I. Yilmaz and M. Sekerci, Journal of Organometallic Chemistry, 692 (2007) 3855-3865.
21. P. R. Shukla, V. K. Singh, A. M. Jaiswal and J. Narain, J. Ind. Chem. Soc., 60 (1983) 321.
22. A. J. Atkins, D. Black, R. L. Finn, A. Marin-Becerra, A.J. Blake, L. Ruiz-Ramirez, W. S. Li and M. Schroder, J. Chem. Soc. Dalton Trans., 9 (2003) 1730.
23. H. P. Ebrahimi, J. S. Hadi, A. Z. Abdulnabi and Z. B. olandnazar, Spectrochim. Acta Part A, 117 (2014) 485-492.
24. S. C. Bajia, Synth. React. Inorg. Met-Org. Nano-Met. Chem., 41 (2011) 746-749.
25. K.M. Ibrahim, R. R. Zaky, E. A. Gomaa and M. N. Abd El-Hady, Spectrochem. Acta Part A, 107 (2013) 133-144.
26. D. A. Galicoa, B. B. C. Holandaa, R. B. Guerraa, A. O. Legendrea, D. Rinaldoa, O. Treu-Filho and G. Bannacha, Thermochim. Acta, 575 (2014) 226-232.
27. K. R. Surati, Spectrochim. Acta Part A, 79 (2011) 272-277.
28. G. J. Kharadi and K. D. patel, Appl. Organometal. Chem., 24 (2010) 523-529.
29. K. S. Abou-Melha, Spectrochim. Acta Part A, 109 (2013) 146-154.
30. N.S. Youssefi and K.H. Hegab, J. Mater. Sci. Technol., 15 (3) (1999) 253.
31. B. Lakshmi, K.N. Shivananda, A.P. Gouda, K.R. Krishna Reddy and K.N. Mahendra, Bull Korean Chem. Soc., 32 (2011) 5.
32. Al-Adilee, K.J. and A. Shaimaa, Oriental Journal of Chemistry, 2017. 33(4): p. 1-14.
33. W. A. Ghanem, Applied Surface Science, 329 (2015) 104-115.
34. A. W. Coats, & J. P. Redfern, J. P. Nature, 201 (1964), 68-69.
35. A. Faheim, & A. M. Alaghaz, Current Synthetic and Systems Biology, 2 (2014) 113 , 1-7.
36. C. R. Vinodkumar, M. K. Muraleedharan Nair, P. K. Radhakrishnan, J. Therm. Anal. Cal. 2000, 61, 143.
37. Z. H. Abd El-Wahab, & A. A. Faheim, Phosphorus, Sulfur, and Silicon and the Related Elements, 184(2) (2009), 341-361.
38. N. O. Obi-Egbedi, I. B. Obot, M. I. El-Khaiary, S. A. Umoren, E. E. Ebenso, Int. J. Electrochem. Sci. 2011, 6, 5649.
39. M. N. Khomami, I. Danaee and A. A. Attar, Transactions of the Indian Institute of Metals, 5 (2012) 303-311.
40. QiufaXu, KeweiGao, WentingLv and Xiaolu Pang, Corrosion Science, 102 (2016)114-124.
41. S. Azumaa, T. Kudob, H. Miyukib, M. Yamashitac and H. Uchidac, Corrosion Science, 46 (2004) 2265-2280.
42. A. A. Faheim, Modern Chemistry, 2 (2014) 10-22.
43. T. Nishimura, H. Katayama, K. Noda and T. Kodama, Corrosion Science, 42 (2000) 1611-1621.
44. P. Bruijninx and P. J. Sadler, Curr. Opin. Chem. Biol., 12 (2008) 197-206.
45. R. Labianca, G.D. Beretta, B. Kildani, L. Milesi, F. Merlin, S. Mosconi, M.A. Pessi, T. Prochilo, A. Quadri and G. Gatta, Crit. Rev. Oncol. Hematol, 74 (2010) 106-133.
46. V. Cutsem, E. Kohne, C.H. Hitre and E. Zaluski, J. Chang Chien, C.R. Makhson, A.; D'Haens, G. Pinter, T.; Lim, R.; Bodoky, G.; et al., N. Engl. J. Med., 360 (2009) 1408-1417.

Please cite this article as Abeer A. Faheim, Dalia I. Saleh and Amal M. Al-Khudaydi, (2019) Biological Activity and Antitumor Studies of Some Metal Complexes with O,N,O- Chelating Schiff's Base Ligand. *International Journal of Recent Research and Applied Studies*, 6- 4(4), 22-35